1988

Analysis of Electrokinetic Data by Parameter Estimation and Model Discrimination Techniques

Prosper K. Adanuvor
Texas A & M University - College Station

Ralph E. White
University of South Carolina - Columbia, white@cec.sc.edu

Publication Info

Journal of the Electrochemical Society, 1988, pages 1887-1898.

http://www.electrochem.org
DOI: 10.1149/1.2096174
http://dx.doi.org/10.1149/1.2096174

Press, Cleveland, OH (1983).
5. W. Parkhurst, R. Freeman, A. J. Salkind, J. Weckesser, S. Dallek, and J. McBreen, Abstract 48, p. 77, The Electrochemical Society Extended Abstracts, Vol. 85-2, Las Vegas, Nevada, Oct. 13-18, 1985.
6. R. W. Freeman, A. J. Salkind, W. A. Parkhurst, and J. Weckesser, Abstract 49, p. 79, The Electrochemical Society Extended Abstracts, Vol. 85-2, Las Vegas, Nevada, Oct. 13-18, 1985.
7. W. West, R. W. Freeman, S. Dallek, and A. J. Salkind, Paper No. 24, 15th International Power Sources Conference, Brighton, Sept. 1986.
8. W. A. Parkhurst, S. Dallek, and B. F. Larrick, *This Journal*, **131**, 1739 (1984).
9. L. J. van der Pauw, *Philips Res. Rep.*, **13**, 1 (1958).
10. R. N. Hammer and J. Kleinberg, in "Inorganic Synthesis," Vol. IV, J. C. Bailar Jr., Editor, pp. 12-13, McGraw-Hill Book Co., New York (1953).
11. S. D. Hottman and H. A. Pohl, *Rev. Sci. Instrum.*, **42**, 387 (1971).
12. C. R. Anderson, W. A. West, A. N. Mansour, M. K. Norr, F. Santiago, and B. F. Larrick, Abstract 736, p. 1086, The Electrochemical Society Extended Abstracts, Vol. 86-2, San Diego, CA, Oct. 19-24, 1986.
13. A. Tvarusko, *This Journal*, **115**, 1105 (1968).
14. T. P. Dirske, in "Zinc-Silver Oxide Batteries," A. Fleischer and J. J. Lander, Editors, pp. 117-131, John Wiley and Sons, New York (1971).
15. S. Dallek, W. A. West, and B. F. Larrick, *This Journal*, **133**, 2451 (1986).
16. S. Dallek, D. R. Glen, K. M. O'Neill, and B. F. Larrick, Abstract 153, p. 222, The Electrochemical Society Extended Abstracts, Vol. 87-2, Honolulu, HI, Oct. 18-23, 1987.

Analysis of Electrokinetic Data by Parameter Estimation and Model Discrimination Technqiues

Prosper K. Adanuvor and Ralph E. White*

Department of Chemical Engineering, Texas A&M University, College Station, Texas 77843

ABSTRACT

An alternative approach to classical methods of electrochemical data analysis is presented. This alternative method is based on nonlinear parameter estimation and model discrimination techniques. The method is used to obtain the relevant kinetic and transport parameters and to elucidate the kinetic mechanism of O_2 reduction at carbon and silver electrodes in alkaline electrolytes.

Conventional methods for electrochemical data analysis generally tend to focus on a narrow range of the kinetic expressions describing the electrochemical process, such as the Tafel or the linear segments of typical polarization curves. Focus on these sections of the polarization curves produces a set of parameter values which electrochemists have traditionally used to elucidate the mechanisms of electrochemical reactions. However, in most instances, the linear and Tafel segments of these curves are distorted by diffusion processes, the reverse reaction in the neighborhood of the equilibrium potential, and coupling effects of other reactions. Therefore, parameters estimated from the Tafel or linear regions of the polarization curves, especially for complex electrode reaction systems, may not reflect the true values of the parameters of the electrode reactions under consideration. For instance, where the electrode reaction is relatively fast, the Tafel segment may be so short as to create difficulty in accurately estimating the parameters. On the other hand, for slow electrode reactions, the polarization curves can have several Tafel segments with transition regions, where the reaction from one segment could be coupled with that in another segment. McIntyre (1) noted the coupling effect of a regenerative process of a heterogeneous catalytic electrode reaction over the complete potential range in which the electroactive species was reduced and recommended that the coupling effect be taken into account if kinetic parameters characteristic of the charge-transfer reaction are to be obtained. On the other hand, the linear region extends only a few millivolts beyond the equilibrium or open-circuit potential. As pointed out by Nagy *et al.* (2), measurements at such low overpotentials are often hampered by signal-to-noise ratio problems, and extrapolation from the linear to higher overpotential range as commonly done in electrochemical studies is generally questionable.

Most kinetic models, in addition to relating the overall process and the component steps to the potential driving force and to the concentrations of reactants, products, and intermediates, must also take into account the transport of reacting species, intermediates, and products to and from the electrode surface. Furthermore, consideration of homogeneous reactions in the solution and heterogeneous non-charge transfer reactions at the electrode surface increases the complexity of the system of model equations needed to evaluate the kinetic parameters. This system of model equations is normally described by a set of differential equations containing the unknown parameters, some of which may enter into the boundary conditions. In classical electrokinetic data analysis, a number of simplifying assumptions are made in order to adapt the problem to analytical solutions (3). This approach tends to limit the kinetic models to a narrow range of the variables over which only a limited number of the parameters can be estimated at once. On the contrary, the development of numerical algorithms for the solution of electrochemical problems (4-7) makes it possible for the investigator to predict the behavior of such complex electrochemical systems over a wide range of the variables. This facilitates the simultaneous estimation of the parameters from experimental data. Consequently, more rigorous kinetic expressions can be developed to cover the range of variables of practical interest.

Only a few attempts have been made to estimate electrokinetic parameters by parameter estimation techniques. A multiparameter least square curve fitting program was developed by Meites and Meites (8). This program was based on a trial-and-error search pattern in which each parameter is successively varied while the others are held constant until the optimum point is reached. This program was applied to problems in titrimetry, polarography, and chronoamperometry, and could estimate up to five parameters. Gorodestskii *et al.* (9) used a nonlinear technique—the method of steepest descent—to estimate the transfer coefficients and exchange current densities of bismuth discharge reactions on a stationary amalgam electrode. Vert and Pavlova (10) used the method of least squares to calculate the exchange current density of the slow step of an electrochemical reaction and the potential correspond-

* Electrochemical Society Active Member.

ing to this current from polarization measurements covering both the Tafel region and the section where the back reaction cannot be neglected. Degreve *et al.* (11) used the Gauss-Newton method to determine the individual electrochemical parameters ($E_{1/2}$, i_d, and αn) from a composite dc polarographic wave. The kinetic models considered by the above investigators (8-11) were based on nonlinear algebraic expressions for the current-potential relationship without consideration of the mass transfer or potential distribution effects on the kinetic models. Caban and Chapman (5) went a step further by using orthogonal collocation to simulate the current-potential values taking into consideration mass transfer and potential distribution effects and minimizing the residual sum of squares of the predicted and observed values to obtain the kinetic parameters. Their technique was used to determine the exchange current density and the transfer coefficient for copper deposition from $CuSO_4$-H_2SO_4 solutions. Nagy (12, 13) presented a series of systematic analyses on data-fitting methods for evaluating electrokinetic parameters derived from a galvanostatic relaxation technique in the linear region. From his analyses, he concluded that numerical curve-fitting, using nonlinear, multidimensional least squares calculation, is the best data evaluation method for all dc relaxation techniques in the linear range. Recently, Nagy *et al.* (2) extended the same curve-fitting techniques into the nonlinear current-potential region in order to overcome problems associated with limiting the relaxation technique to the linear potential region.

In general, the application of numerical curve-fitting techniques in electrochemistry has either been limited to simple electrode systems (5, 8-13) or the numerical algorithms for the curve-fitting procedure have not necessarily been the most efficient (8-13). For example, as a general rule, search techniques as employed by Meites and Meites (8) converge rather slowly when compared to the derivative-type techniques, although search methods do not require continuity and the existence of derivatives for the objective function. Newton's method as employed by Gorodeski *et al.* (9) exhibits a quadratic convergence in the vicinity of the minimum but behaves poorly further from the minimum, which is the region that the steepest descent method employed by Degreve *et al.* (11) performs the best. Therefore, a combination of the two methods (the steepest descent and Newton's methods) should exhibit superior performance to either method—an important feature of the Levenberg-Marquardt algorithm (14, 15). The Levenberg-Marquardt algorithm is a fast and reliable technique for evaluating unconstrained nonlinear least squares problems. Nagy *et al.* (2) recommend that this algorithm with the capability to handle constraints be used for nonlinear least squares problems.

In this paper, a parameter estimation procedure based on Levenberg-Marquardt algorithm is developed to handle a system of complex electrochemical reactions. The procedure consists of making initial guesses of the parameters and then proceeding to simulate the current-potential data, taking into consideration mass transfer and potential distribution effects in the solution, the occurrence of homogeneous reactions in the solution or heterogeneous noncharge transfer reactions at the electrode surface with associated parameters, and the possibility of multiple reactions at the electrode surface. The simulated current-potential data are compared to experimental data and subjected to a least squares minimization procedure based on the Levenberg-Marquardt algorithm (15) through an iterative scheme that updates the parameters until all the convergence criteria are satisfied.

To illustrate this technique, the procedure is applied to a set of experimental data on oxygen reduction at carbon and silver electrodes. Since the reduction of oxygen can occur via a number of possible reaction mechanisms (16), statistical model discrimination techniques are used to determine which mechanism best describes a given set of experimental data. The parameter values obtained from the best model fit to the data are compared to other values (calculated by other techniques or obtained from the literature) in order to assess the performance of this alternative method for electrokinetic data analysis.

Simulation of electrochemical reactions at a rotating disk electrode.—The optimization approach outlined in this paper consists of a model that can be used to predict values of the current density as a function of the applied potential. The deviations between the model predicted and experimentally observed values of the current density are then minimized through the application of Levenberg-Marquardt algorithm (15) which progressively updates the parameter values until the convergence criteria are satisfied.

Several models for simulating electrochemical reactions at a rotating disk electrode have been presented in the literature (4-7, 17). For this reason, only a brief outline of the set of governing equations necessary to define the relevant terms in the optimization procedure will be given here.

From Ref. (4) and (17), a material balance on a volume element of a steady flow of an incompressible fluid caused by the rotation of a large circular disk about its central axis yields a set of coupled ordinary differential equations as follows

$$D_i \frac{d^2c_i}{d^2\xi} + 3D_R\xi^2 \frac{dc_i}{d\xi} + z_i\mathbf{F}\frac{D_i}{RT}\left(\frac{d\Phi}{d\xi}\frac{dc_i}{d\xi} + c_i\frac{d^2\Phi}{d^2\xi}\right) + \delta_D{}^2R_i = 0 \quad [1]$$

where R_i, the homogeneous reaction rate in the solution, can be expressed as (18)

$$R_i = k_f\mu_i\left(\prod_{\mu_i>0} c_i{}^{\mu_i} - \frac{1}{K_{eq}}\prod_{\mu_i<0} c_i{}^{-\mu_i}\right) \quad [2]$$

in which μ_i is the stoichiometric coefficient for species i, and k_f and k_b are the forward and backward rate constants for the homogeneous reaction. k_f and k_b are parameters that can be estimated from the proposed optimization procedure. Actually, one needs to determine k_f only because k_b can be obtained from the equilibrium relationship in Eq. [3]. If the species M_i were electrochemically inactive, all the $M_1, \ldots, M_N$ species in the solution would be in equilibrium, obeying the relation

$$\prod_i c^{\mu_i}{}_{i,bulk} = k_f/k_b = K_{eq} \quad [3]$$

where $c_{i,bulk}$ is the bulk concentration of species i and K_{eq} is the equilibrium constant. On the other hand, if a species is assumed to be electrochemically active, it can react at the electrode according to the general relation

$$\sum_i^m s_{ij}M_i{}^{z_i} \rightarrow n_je^- \quad [4]$$

The dimensionless distance is defined as

$$\xi = y/\delta_D \quad [5]$$

where y is the normal distance from the electrode surface and where δ_D is the diffusion layer thickness. δ_D is related to the rotation speed of the electrode by the relation (19)

$$\delta_D = \left(\frac{3D_R}{a\nu}\right)^{1/3}\left(\frac{\nu}{\Omega}\right)^{1/2} \quad [6]$$

The boundary conditions are as follows:

In the bulk solution (bulk conditions are presumed to exist at $\xi \geq 2\delta_D$, since a significant proportion of the change in concentration or potential occurs in the diffusion layer [see Ref. (19) p. 306])

$$\text{at } \xi = 2 \quad c_i = c_{i,bulk} \text{ and } \Phi = \Phi_{re} \quad [7]$$

where

$$c_{i,bulk} = \begin{cases} c_{i,re} + \mu_i\epsilon_i, & \text{if } i \text{ is involved in a homogeneous reaction;} \\ c_{i,re} & \text{otherwise} \end{cases} \quad [8]$$

ϵ_i is the degree of dissociation or association of species i

and is calculated from Eq. [3]. At the electrode surface, as $\xi \rightarrow 0$, $\Phi \rightarrow \Phi_o$, and

$$\frac{1}{\delta_D}\left[D_i\frac{dc_i}{d\xi} + z_i c_i \mathbf{F}\frac{D_i}{RT}\frac{d\Phi}{d\xi}\right]_{|\xi=o} = \sum_{j=1}^{m}\frac{s_{ij}i_j}{n_j\mathbf{F}} + \sum_{l=m+1}^{nr} s_{il}r_{i,l} \quad [9]$$

$r_{i,l}$ in Eq. [9] represents a non-charge transfer reaction at the electrode surface, whose reaction rate can be expressed in terms of the disappearance of species i by

$$r_{i,l} = -k_{h,l}c_i^p \quad [10]$$

where $k_{h,l}$ is the rate constant for reaction l and is included here as a parameter to be estimated. The reaction order p is assumed typically to be known from independent experimental measurements. The local current density term, i_j, in Eq. [11] is usually approximated by the Butler-Volmer equation with p_{ij} and q_{ij} as the anodic and cathodic reaction orders

$$i_j = i_{oj,ref}\left[\left(\frac{c_{i,o}}{c_{i,ref}}\right)^{pij}\exp\left(\frac{\alpha_{aj}\mathbf{F}}{RT}\eta_j\right) - \left(\frac{c_{i,o}}{c_{i,ref}}\right)^{qij}\exp\left(\frac{-\alpha_{cj}\mathbf{F}}{RT}\eta_j\right)\right] \quad [11]$$

which, in the examples discussed in this paper, are assumed to be known, although, they could be determined by the technique outlined here. The exchange current density $i_{oj,ref}$ at the reference concentration, $c_{i,ref}$, of species i and the apparent transfer coefficients, $\alpha_{a,j}$ and $\alpha_{c,j}$ complete the list of kinetic parameters to be estimated. It must be noted that the form of the kinetic expression used in Eq. [11] requires that (20)

$$\alpha_{a,j} + \alpha_{c,j} = n_j \quad [12]$$

in which case, only $\alpha_{a,j}$ or $\alpha_{c,j}$ needs to be estimated since n_j is presumed to be known from independent analysis. The total current density is the sum of the partial current densities, that is

$$i = \sum_j i_j \quad [13]$$

and the overpotential is

$$\eta_j = \Phi_{met} - \Phi_{re} - (\Phi_o - \Phi_{re}) - U_{j,ref} \quad [14]$$

in which the applied potential, E_{appl} is given by $\Phi_{met} - \Phi_{re}$. The standard potential of reaction j with respect to the reference solution concentration is given by

$$U_{j,ref} = U_j^\theta - U_{re}^\theta - \frac{RT}{n\mathbf{F}}\sum_i s_{ij}\ln\left(\frac{c_{i,ref}}{\rho_o}\right) + \frac{RT}{n_{re}\mathbf{F}}\sum_i s_{i,re}\ln\left(\frac{c_{i,re}}{\rho_o}\right) \quad [15]$$

Experimentally, under potentiostatic conditions, the net current density i is measured at specified values of E_{appl}. The transport parameters, the diffusion coefficient of the limiting reactant, D_R, and perhaps the diffusion coefficients of other components are also potential candidates for the parameter estimation procedure if their values are not already available from independent measurements. A number of parameters or characteristics have to be specified before numerical results can be obtained. These are as follows: m, n_j, nr, ρ_o, ν, Ω, s_{ij}, T, Φ_{met}, Φ_{re}, ξ at the location of the reference electrode, and the type of reference electrode. Numerical solution of this system of coupled ordinary nonlinear differential equations is obtained by a procedure outlined in a previous paper (4). The solution yields predicted current density values, i, at specified values of E_{appl}. These predicted values are then compared with the corresponding experimental values and subjected to the parameter estimation process to yield the optimum values of the parameters.

Parameter estimation procedure.—In general, nonlinear parameter estimation or optimization problems necessarily have many possible solutions. The aim of optimization is to determine the best possible solution from among other potential solutions under consideration, subject to some performance criteria. The procedure outlined in this paper deals with unconstrained nonlinear least squares problems. The method of obtaining the optimum estimates of the vector of parameters $\mathbf{x}$ consists of minimizing the sum of squares of the weighted deviations between the observed and predicted values as defined by the objective function

$$F(\mathbf{x}, t) = \sum_{k=1}^{n} w_k[y_{k,obs} - f_k(\mathbf{x}, t)]^2 = \sum_{k=1}^{n} w_k\mathbf{e}_k^2 \quad [16]$$

where $\mathbf{e}_k = y_{k,obs} - f_k(\mathbf{x}, t)$. $y_{k,obs}$ and f_k are respectively the observed and the expected values of the dependent variable, w_k is the weight attached to the k^{th} observed value (w_k was taken to be unity in our computations), and t is the independent variable. A number of gradient methods have been developed to reduce significantly the computational effort necessary to determine the optimum parameters (14, 15). The important steps of these methods reduce to making an initial guess of the vector of parameters $\mathbf{x}^1$ and then proceeding iteratively to generate a sequence of values $\mathbf{x}^2$, $\mathbf{x}^3$, $\mathbf{x}^4$, ... according to

$$\mathbf{x}^{j+1} = \mathbf{x}^j + \Delta\mathbf{x}^j \quad [17]$$

which it is hoped will converge to the point $\mathbf{x}^*$, where $F(\mathbf{x}^*, t)$ is the minimum. The displacement vector, $\Delta\mathbf{x}_k^j$, is determined by exploiting the nature of the objective function. For example, for second derivative methods

$$\Delta x^j = [\mathbf{H}^j]^{-1}\,\mathbf{q}^j \quad [18]$$

where

$$q_\alpha{}^j = \frac{\partial F^j}{\partial x_\alpha} = 2\sum_{k=1}^{n} w_k{}^j e_k{}^j\frac{\partial e_k{}^j}{\partial x_\alpha} = -2\sum_{k=1}^{n} w_k{}^j e_k{}^j\frac{\partial f_k{}^j}{\partial x_\alpha} \quad [19]$$

and

$$H_{\alpha\beta}{}^j = \frac{\partial^2 F^j}{\partial x_\alpha \partial x_\beta} = -2\sum_{k=1}^{n} w_k{}^j e_k{}^j\frac{\partial^2 f_k{}^j}{\partial x_\alpha \partial x_\beta} + 2\sum_{k=1}^{n} w_k{}^j\frac{\partial f_k{}^j}{\partial x_\alpha}\frac{\partial f_k{}^j}{\partial x_\beta} \quad [20]$$

If the residual in the first term of Eq. [19] is assumed to be small, this term can be ignored to give the Gauss-Newton approximation to the Hessian matrix.

$$H_{\alpha\beta}{}^j = 2\sum_{k=1}^{n} w_k{}^j\frac{\partial f_k{}^j}{\partial x_\alpha}\frac{\partial f_k{}^j}{\partial x_\beta} \quad [21]$$

However, the objective function, $F^j(\mathbf{x}, t)$, is guaranteed to converge to the minimum only if the Hessian is positive definite. The Levenberg-Marquardt method suggests the addition of a positive constant, λ_o, to Eq. [21] to insure that the Hessian matrix is positive definite. Therefore, at the j^{th} iteration step

$$\mathbf{N}^j = -(\mathbf{H}^j + \lambda_o{}^j\mathbf{I}^j) \quad [22]$$

where $\lambda_o{}^j$ is chosen to insure the descent direction at step j of the iteration and $\mathbf{N}^j$ replaces $\mathbf{H}^j$ in Eq. [18]. Equation [22] combines the steepest descent and Gauss-Newton methods (14, 15), taking advantage of the early convergence of the steepest descent method ($\lambda_o \rightarrow \infty$) further away from the minimum, while automatically switching to the Gauss-Newton method ($\lambda_o \rightarrow 0$) near the minimum where the latter exhibits quadratic convergence.

Evaluation of the derivatives for the optimization procedure.—The solution of the model equations in Eq. [1-14] yields values of the dependent variable, i, as a function of the independent variable E_{appl}. The parameters $\alpha_{c,j}$ (or $\alpha_{a,j}$) and $i_{oj,ref}$ occur directly in the expressions for the dependent variable in Eq. [13]. However, D_i, k_h, and k_f appear only

indirectly in the expression in Eq. [13] for the dependent variable. The latter expressions depend explicitly on the model equations which, in turn, depend on the parameters D_i, k_h, and k_f.

Two methods were used to obtain the approximate derivatives for evaluating the gradient vector, **q**, and the Hessian matrix, **N**, both of which are needed to evaluate the displacement vector in Eq. [18]. The first method was by the finite-difference approximation. This method was used to evaluate the derivatives of parameters such as D_i, k_h, and k_f that have an indirect dependence on the dependent variable, i. The second method was the direct analytical approach. This method was used to obtain the derivatives of those parameters with direct dependence on the dependent variable by direct differentiation of the dependent variable with respect to the parameters to generate an additional set of ordinary differential equations. For example, the derivative for the parameter, $i_{oj,ref}$, can be obtained by differentiating Eq. [13] with respect to the parameter, that is, $\partial i/\partial i_{oj,ref}$, to create an additional ordinary differential equation. This additional equation neglects the indirect dependence of the concentration and potential terms on the parameter, that is, $\partial c(x, t)/\partial i_{oj,ref}$ and $\partial \Phi(x, t)/\partial i_{oj,ref}$. In a similar manner, the derivatives of the parameters $\alpha_{c,j}$ can be evaluated by the direct analytical approach. Evaluation of all the derivatives by the forward difference approximation would require $N + 1$ additional evaluation of the model differential equations, resulting in increased computational effort and time. On the other hand, the analytical approximation adds $N + 1$ extra ordinary differential equations to the model equations and solves the set of model differential equations once for the $N + 1$ derivatives obtained by this technique. Thus, with the latter approach there could be considerable savings in the time and effort needed to compute the derivatives. However, the inherent error in the analytical approach as a consequence of neglecting the indirect dependence of the concentration or potential terms on the parameters could lead to serious problems in the evaluation of the derivatives under certain conditions. Nevertheless, a combination of the analytical approach with the finite difference approximation for the case where all the derivatives cannot be evaluated by the analytical approach may offer some advantages over the finite difference approach under certain conditions.

Parameter interaction.—A problem encountered with the least squares minimization of the objective function defined in Eq. [16] was the high degree of interaction between some of the parameters, typically between $\alpha_{c,j}$ (or $\alpha_{a,j}$) and $i_{oj,ref}$. This could lead to singularity of the Hessian matrix and as a result, to convergence difficulties under certain conditions. To remove the interaction between $\alpha_{c,j}$ (or $\alpha_{a,j}$) and $i_{oj,ref}$, the model equation as expressed in Eq. [13] was transformed to

$$i_j = \left(\frac{c_{i,o}}{c_{i,ref}}\right)^{p_{ij}} \exp\left\{\hat{i}_{oj} + \frac{(n_j - \alpha_{c,j})\mathbf{F}}{RT}\eta_j\right\} - \left(\frac{c_{i,o}}{c_{i,ref}}\right)^{q_{ij}} \exp\left\{\hat{i}_{oj} - \frac{\alpha_{c,j}\mathbf{F}}{RT}\eta_j\right\} \quad [23]$$

where $\hat{i}_{oj} = \ln(i_{oj,ref})$ and $n_j - \alpha_{c,j} = \alpha_{a,j}$. Thus, $\hat{i}_{oj}$ becomes the parameter to estimate. From the estimate of $\hat{i}_{oj}$, $i_{oj,ref}$ can be obtained by application of the inverse log transformation.

Parameter scaling.—Typical values of the parameters in question ranged from 1.0×10^{-6} cm^2/s for D_i to 1.0×10^4 cm/s for $k_{h,j}$. Because the parameters differ greatly in order of magnitude, the optimization process becomes insensitive to changes in the values of the parameters in the small terms. To alleviate this problem, all the parameters are scaled to about the same order of magnitude; in this case, that is $0 < x_j \leq 2$.

Confidence region for the parameter estimates.—In addition to estimating the parameters in the model, it is important to obtain some measure of dispersion of the parameter estimates. Approximate confidence regions for the individual parameters can be constructed by linearizing the nonlinear model about the least squares estimates in the parameter space (21). For γ significance level and df degrees of freedom, the individual parameter confidence intervals can be computed from the following expression as given previously (21)

$$\hat{x}_j - t_{1-\gamma/2}\sqrt{\mathrm{Var}\{x_j\}} \leq x_j \leq \hat{x}_j + t_{1+\gamma/2}\sqrt{\mathrm{Var}\{x_j\}} \quad [24]$$

where $\hat{x}_j$ is the estimate of the parameter x_j, $\mathrm{Var}\{x_j\}$ the variance of x_j, and $t_{1-\gamma/2}$ the t-distribution at $(1 - \gamma/2)$ percent confidence interval and at df degrees of freedom.

Sensitivity of the estimates.—Before implementing the optimization routine to obtain the optimum values of the parameters, it is important to perform *a priori* a sensitivity analysis of all the parameters that are candidates for estimation. Sensitivity analysis is performed on the parameters to assess quantitatively the relative sensitivity of the objective function to changes in the parameter values. Following the approach of Himmelblau (21) and White *et al.* (22), the relative sensitivity is determined by the absolute value of the normalized derivatives of the objective function with respect to each parameter, q_j, by the relationship

$$\bar{q}_j = \left|\frac{x_j}{F(x, t)\, q_j}\right| \quad [25]$$

By comparing the relative gradient values, $\bar{q}_j$ it becomes easier to determine those parameters with the dominant influence on the objective function. Also, it makes it possible to eliminate any parameters from the initial list of parameters to be estimated if the objective function is found to be insensitive to changes in that particular parameter. In this way considerable computational effort and time can be saved in implementing the optimization routine. However, a concerted effort must be made to provide reasonable values for the parameters that are eliminated *a priori* through independent experimental measurements or from the literature.

Implementation of parameter estimation technique.—A computer code based on the Levenberg-Marquardt algorithm was written to carry out the minimization of the objective function. The computer code obtains the optimum parameter estimates, the confidence interval for these parameters, and the relative sensitivity of each parameter estimate at the optimum point. The code performed relatively well (20) against the IMSL subroutine code-named ZXSSQ (23), when applied to the same test problems. In the application of the code developed here to experimental data, some modifications were introduced in order to decrease the time necessary to achieve convergence of the procedure and to improve the chances of the procedure terminating at a global minimum. In principle, the more reasonable the initial guesses of the parameters, the quicker the convergence. In general, initial guesses of the parameters were made on physical grounds—on the basis of earlier kinetic studies of similar systems in the literature or through the application of classical electrochemical data analysis techniques such as Tafel plots or the Levich equation. In cases where no information was available, reasonable values are assumed. Another technique used to refine the initial guesses was to make contour plots of the objective function as a function of at least two parameters, while holding all other parameters constant.

To accelerate convergence of the routine, it was necessary to place some restriction on some of the parameters. These restrictions were imposed as a result of the electrochemical properties of the parameters rather than as a condition for implementation of the proposed algorithm. For example, $\alpha_{c,j}$ was restricted to between zero and n_j, that is $0 \leq \alpha_{c,j} \leq n_j$, and $i_{oj,ref}$ and D_i was restricted to $i_{oj,ref} > 0$ and $D_i > 0$.

Model discrimination procedure.—To provide a statistical basis for discriminating between models, the test developed by Wilks (24, 25, 21) for comparing several linear or nonlinear estimated regression equations simultaneously was used. On the basis of the fact that for a single estimated regression equation an F-test, based on analysis of variance, can be applied as an overall test of significance

of regression, Wilks (24) proposed that by extension, the F-test can be used to discriminate among different estimated regression equations if they are assembled in a linear combination as follows

$$\hat{Y}^* = b_1^*\hat{Y}_1 + b_2^*\hat{Y}_2 + \ldots + b_p^*\hat{Y}_p \quad [26]$$

where $\hat{Y}^*$ is a linear combination of the various regression equations $\hat{Y}_1, \hat{Y}_2, \ldots, \hat{Y}_p$. The b^*'s are chosen so that each regression equation contributes toward Y^* according to its fitness as an estimator of $\hat{Y}^*$. For convenience, the b^*'s are adjusted so that $\sum_{k=1}^{p} b_k^* = 1$. Once the b^*'s are computed (see Ref. (21) for a summary of the computational procedure), their order of rank is a rough measure of the effectiveness of each regression equation in fitting the experimental data. Furthermore, any two b^*'s can be tested in order to determine whether there is any significant difference between them, and for that matter, to determine whether one estimated regression equation is better than the other. The null hypothesis is that the two regression models are of equal ability in predicting the value of the dependent variable, Y^*'s. To test for a difference between the two parameters b_j^* and b_k^* (or the two regression equations), a t value is computed as follows

$$t = \frac{b_j^* - b_k^*}{\sqrt{\mathrm{Var}(b_j^*) + \mathrm{Var}(b_k^*) - 2\mathrm{Covar}(b_j^*, b_k^*)}} \quad [27]$$

For a significance level of γ, if t is greater than $t_{1-\gamma/2}$ obtained from the table of the t distribution at $n-p+1$ degrees of freedom, the null hypothesis is rejected. Therefore, it can be concluded that b_j^* and b_k^* are different and $\hat{Y}_j$ is a better fit to the model than $\hat{Y}_k$, when $b_j^* > b_k^*$.

Results and Discussion

The optimization procedure was applied to real experimental data as opposed to simulated data (2). The system chosen to demonstrate this procedure was the reduction of O_2 in alkaline electrolytes. Cathodic reduction of O_2 is a complex electrochemical process that proceeds through a series of parallel, consecutive, reversible, charge transfer, and noncharge transfer reactions as shown below.

$$O_2 + 2H_2O + 4e^- \rightarrow 4\ OH^- \qquad U_1^\theta = +0.401V \quad [28]$$

$$O_2 + H_2O + 2e^- \rightleftharpoons HO_2^- + OH^- \qquad U_2^\theta = -0.0649V \quad [29]$$

$$HO_2^- + H_2O + 2e^- \rightarrow 3\ OH^- \qquad U_3^\theta = +0.867V \quad [30]$$

$$HO_2^- \rightarrow OH^- + 1/2\ O_2 \qquad \Delta G^\circ_{298} = -184.09\ \mathrm{kJ/mol} \quad [31]$$

Depending on the nature of the electrode material, the electrolyte, and the operating conditions, various combinations of reaction schemes for oxygen reduction are possible (26). Table I illustrates possible reaction schemes for O_2 reduction in alkaline electrolytes. The technique outlined in this paper provides a basis for distinguishing among the reaction schemes and selecting the scheme that best describes the experimental data.

A priori sensitivity analysis of the electrochemical parameters.—Before attempting to estimate the parameters of the electrochemical system of reactions by the parameter estimation technique, it is necessary to perform *a priori* a sensitivity analysis of the dependent variable with respect to the parameters. This can be carried out by calculating the fractional change in the dependent variable, i, produced by a fractional change in the parameter, x_j, by Eq. [25], for a range of values of the parameter. The parameters of interest in this case are $i_{oj,ref}$, $\alpha_{c,j}$, $k_{h,4}$, D_{O_2}, and $D_{HO_2^-}$, where j = 1,2,3,4 refers to reactions [28] to [31], respectively. The kinetic model for oxygen reduction chosen for *a priori* sensitivity analysis was kinetic model A, the comprehensive model for oxygen reduction. Sensitivity analysis assists in the design of experiments. By collecting data in the region where the objective function or for that matter the dependent variable is most sensitive to changes in the parameters of interest, the experimenter can obtain more efficient estimates of these parameters. Also, sensitivity analysis helps to establish which parameters have no observable effect on the dependent variable in the range in which the data are collected. *A priori* elimination of such parameters from the list of the parameters to be estimated is important in improving the efficiency of implementing the parameter estimation procedure.

In classical data analysis methods, the parameters are normally evaluated from three distinct regions of the polarization curves: the linear, the Tafel, and the limiting current regions (27). For this reason, to implement the sensitivity analysis procedure, three distinct potential values of −0.03, −0.30, and −1.00V with respect to the SCE reference electrode were chosen to coincide with the linear, the Tafel, and the limiting current regions of the polarization curve. Values of the fractional change in the dependent variable with respect to a fractional change in the scaled parameter as specified in Table II for kinetic model A were plotted against scaled parameter values to generate the sensitivity plots in Fig. 1-3. In the lower potential region, as demonstrated in Fig. 1A, the maximum sensitivity occurs with respect to $\alpha_{c,1}$ and $\alpha_{c,3}$. A slight change in these parameters causes a significant change in the dependent variable. However, the high sensitivity with respect to these parameters is limited to a narrow range of parameter values as indicated by the maxima in the sensitivity curves in Fig. 1A. In Fig. 1B, the sensitivity with respect to the reference exchange current densities is quite high and increases steadily over nearly the whole range of parameter values. On the contrary, the sensitivity is quite low with respect to $\alpha_{c,2}$ and D_{O_2}, with the values for $D_{HO_2^-}$ and $k_{h,4}$ being only moderately higher. What this means is that the parameters that can be estimated most efficiently in this region are $\alpha_{c,1}$, $\alpha_{c,3}$, and $i_{oj,ref}$ for j = 1,2, and 3. The sensitivity plots in Fig. 1 indicate moderate sensitivity of the dependent variable to several parameters within the same range of

Table I. Possible reaction schemes for O_2 reduction in alkaline electrolytes

Kinetic model	Reaction scheme	Model description
A	$O_2 + 4H_2O + 4e^- \rightarrow 4\ OH^-$ $O_2 + H_2O + 2e^- \rightleftharpoons HO_2^- + OH^-$ $HO_2^- + H_2O + e^- \rightarrow 3\ OH^-$ $HO_2^- \rightarrow 1/2\ O_2 + OH^-$	Comprehensive model
B	$O_2 + 4H_2O + 4e^- \rightarrow 4\ OH^-$ $O_2 + H_2O + 2e^- \rightleftharpoons HO_2^- + OH^-$ $HO_2^- + H_2O + 2e^- \rightarrow 3\ OH^-$	Parallel mechanism without catalytic decomposition of HO_2^-
C	$O_2 + H_2O + 2e^- \rightleftharpoons HO_2^- + OH^-$ $HO_2^- + H_2O + 2e^- \rightarrow 3\ OH^-$ $HO_2^- \rightarrow 1/2\ O_2 + OH^-$	Sequential mechanism with catalytic HO_2^- decomposition
D	$O_2 + H_2O + 2e^- \rightleftharpoons HO_2^- + OH^-$ $HO_2^- + H_2O + 2e^- \rightarrow 3\ OH^-$	Sequential mechanism without catalytic HO_2^- decomposition
E	$O_2 + H_2O + 2e^- \rightleftharpoons HO_2^- + OH^-$	$2e^-$ reduction to HO_2^- only
F	$O_2 + H_2O + 2e^- \rightleftharpoons HO_2^- + OH^-$ $HO_2^- \rightarrow 1/2\ O_2 + OH^-$	$2e^-$ reduction to HO_2^- with catalytic HO_2^- decomposition
G	$O_2 + 4H_2O + 4e^- \rightarrow 4\ OH^-$	Direct $4e^-$ reduction

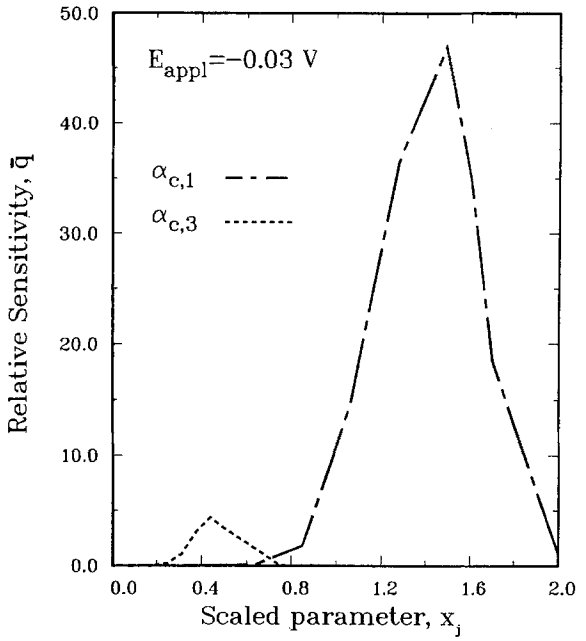

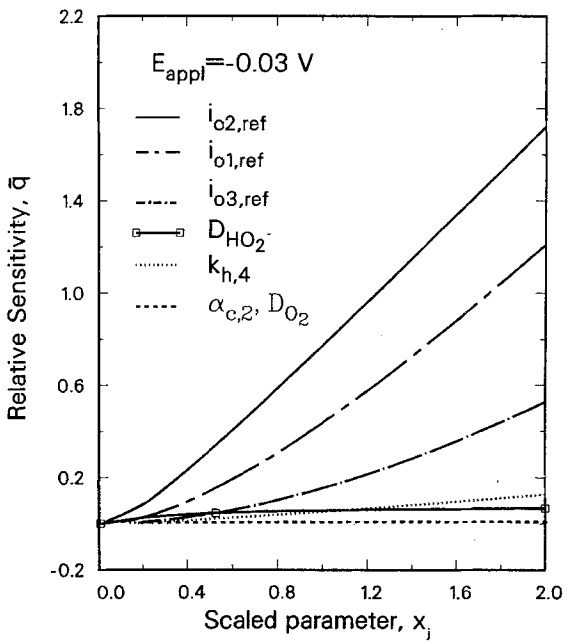

Fig. 1. (A, top) *A priori* sensitivity analysis in the lower potential region. Parameters: $\alpha_{c,1}$, $\alpha_{c,3}$. (B, bottom) *A priori* sensitivity analysis in the lower potential region. Parameters: $i_{o1,ref}$, $i_{o2,ref}$, $i_{o3,ref}$, $D_{HO_2^-}$, $k_{h,4}$, $\alpha_{c,2}$, D_{O_2}.

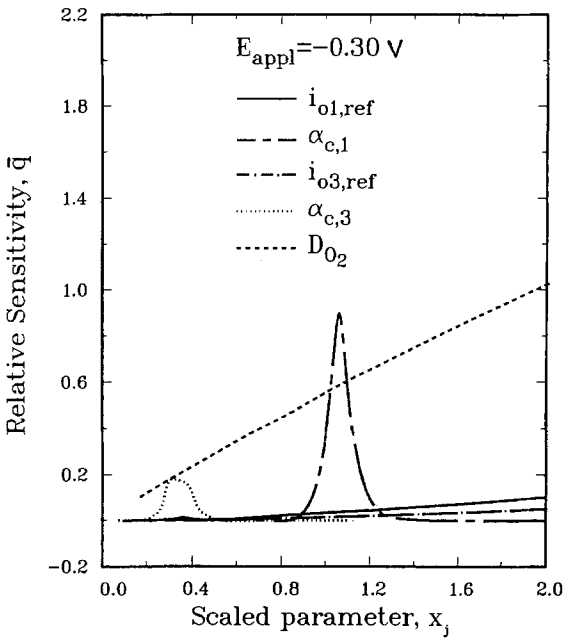

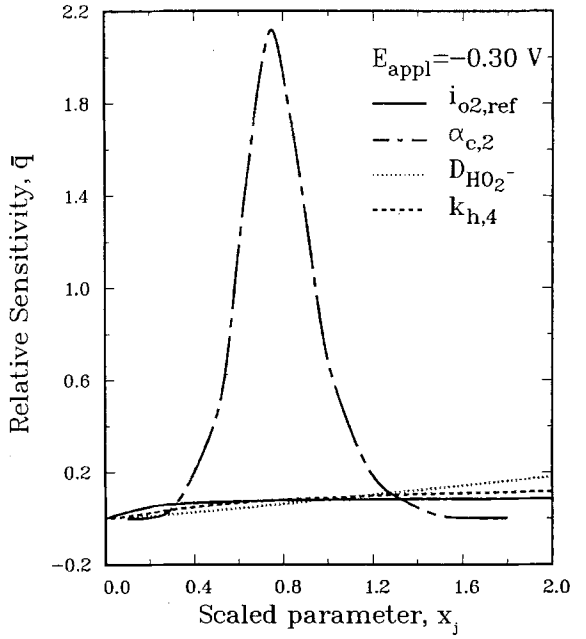

Fig. 2 (A, top) *A priori* sensitivity analysis in the intermediate potential region. Parameters: $i_{o1,ref}$, $i_{o3,ref}$, $\alpha_{c,1}$, $\alpha_{c,3}$, D_{O_2}. (B, bottom) *A priori* sensitivity analysis in the intermediate potential region. Parameters: $i_{o2,ref}$, $D_{HO_2^-}$, $k_{h,4}$, $\alpha_{c,2}$.

parameter values; this makes it more difficult to estimate accurately the individual parameters. In Fig. 2A and 2B, the highest sensitivity occurs with respect to $\alpha_{c,2}$ when the magnitude of the latter lies between 0.4 and 1.2, with the maximum sensitivity occurring around 0.8. Outside this range of values, the dependent variable is for all practical purposes insensitive to changes in $\alpha_{c,2}$. In a similar manner, $\bar{q}$ is very sensitive to changes in $\alpha_{c,2}$ in the range 0.9-1.2. On the other hand, the sensitivity with respect to D_{O_2} increases steadily with increase in the magnitude of this parameter; $\alpha_{c,3}$ shows a moderate increase in sensitivity of i for $0.25 \leq \alpha_{c,3} \leq 0.50$. The parameters $D_{HO_2^-}$, k_h, $i_{o2,ref}$, $i_{o1,ref}$, and $i_{o3,ref}$ also exhibit slight increases in their sensitivity with increase in the values of these parameters. The Tafel region is probably the most common region of the polarization curve used in evaluating the parameters, $\alpha_{c,j}$ or $(\alpha_{a,j})$ and $i_{oj,ref}$. As shown previously (26) for a complex electrochemical reaction as illustrated by the oxygen reduction reaction, the parameters for this system interact and couple with each other over the whole range of parameter values. This creates difficulties in accurately estimating the individual parameters if coupling and interaction effects of other parameters are not taken into account. For example, in conventional data analysis, this region is normally described by the Tafel equation, but as shown in Fig. 2A and 2B, the dependent variable in this region is sensitive to other parameters as well, particularly D_{O_2}. Therefore, if the interaction of other parameters on the transfer coefficients or on the exchange current densities is not removed, exaggerated values of these parameters will normally be obtained from the Tafel equation.

In the diffusion limiting region, only three parameters, D_{O_2}, $D_{HO_2^-}$, and $\alpha_{c,3}$ show any effect at all on the sensitivity calculations as shown in Fig. 3. Also, D_{O_2} has the most dominant influence on $\bar{q}$ in this region. The sensitivity increases in direct proportion to increase in the value of D_{O_2}; however, $D_{HO_2^-}$ and $\alpha_{c,3}$ exhibit a less drastic effect on the sensitivity in this region. The other parameters show practically no effect on the sensitivity analysis in this region. The predominance of D_{O_2} on the sensitivity analysis in this region makes it possible to estimate D_{O_2} more accurately from this region without undue interference from the

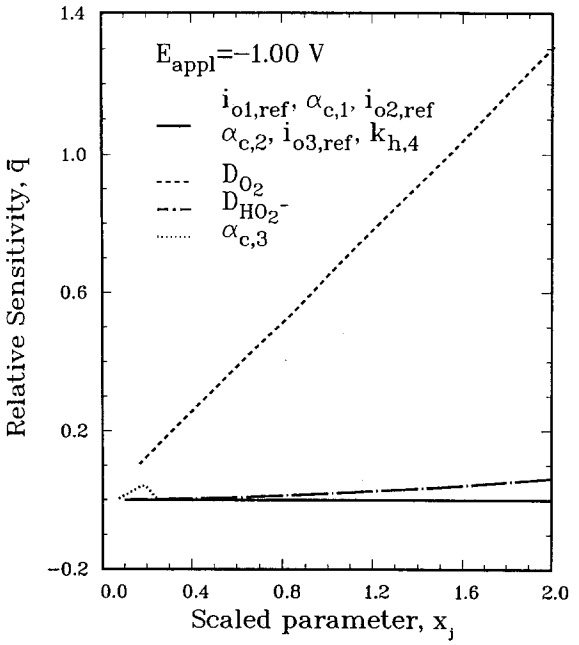

Fig. 3. *A priori* sensitivity analysis in the upper potential region. Parameters: $i_{o1,ref}$, $i_{o2,ref}$, $i_{o3,ref}$, $\alpha_{c,1}$, $\alpha_{c,2}$, $\alpha_{c,3}$, $k_{h,4}$, $D_{HO_2^-}$, D_{O_2}.

other parameters.

The plots in Fig. 1-3 serve a useful purpose because they define regions on the polarization curve where the dependent variable is most sensitive to changes in individual parameters. The significance of this comes into play when the choice of initial guesses has to be made in order for the objective function to converge more rapidly to the optimum point. If the fit to the data is not very good in a particular region, the initial guesses must be modified to reflect the parameters most sensitive to changes in the objective function in that region. The preceding analysis serves as a useful guide in assessing the effect of the individual parameters on the polarization curves. Also, the above analysis illustrates the drawbacks of conventional data analysis techniques such as the application of Tafel plots and the Levich equation to the analysis of complex reaction systems. In any given region of the polarization curve, significant interaction among several parameters occurs. As a result of this, it becomes increasingly difficult to estimate the individual parameters to any high degree of accuracy if the technique is unable to deal with the interaction among the parameters, as is the case with conventional data analysis methods.

Evaluation of electrochemical parameters from polarization data by parameter estimation techniques.—The parameter estimation code developed in our Laboratory was applied to experimental data for oxygen reduction on carbon and silver. The polarization data were obtained by digitizing the experimental polarization curves obtained from the literature in order to gather a sufficient number of *i vs.* E_{appl} data points, typically between 25 and 50 pairs of data uniformly distributed over the whole range of the polarization curve. The experimental *i vs.* E_{appl} data points were then subjected to the optimization process in order to provide accurate estimates of the electrochemical parameters. No attempt was made to correct for any IR drop in the data.

Cathodic polarization of O_2 on pyrolytic carbon electrode.—The first reaction system analyzed with the parameter estimation code was the data of Yeager *et al.* (28) for the cathodic reduction of oxygen on pyrolytic carbon electrode. The disk area of the electrode was given as 0.18 cm^2, and the solution concentration was 4.0*M* with respect to OH^- and 0.016*M* with respect to HO_2^- at 25°C. The partial pressure of oxygen was 0.97 atmosphere. The model proposed by Yeager and his group (28) for this system was model E in Table I, the reduction of O_2 to peroxide stage only.

This model was selected on the basis of the fact that the reduction of O_2 on carbon occurs via the two-step peroxide mechanism and, in tests performed with peroxide solutions with no appreciable amount of O_2 in the solution, the current densities associated with peroxide reduction by Eq. [30] were found to be small compared with those associated with reaction [29]. Not withstanding the low current densities associated with reaction [30], a decision was made to test the two models E and D in order to determine which one of them describes the experimental polarization data better.

The initial estimates of parameters $i_{o2,ref}$, $\alpha_{c,2}$, and D_{O_2} were obtained by conventional analysis of the data via Tafel plots and the Levich equation, while the estimates of $i_{o3,ref}$ and $\alpha_{c,3}$ were made from contour plots of the objective function. It must be emphasized that these initial starting values are in no way unique in locating the minimum since, in general, the objective function tends to be multi-nodal. Therefore, it is important that the optimization procedure be implemented with different sets of reasonable starting values in order to improve the chances of the procedure coverging to a global minimum. A set of values of the initial guesses of the parameters to be estimated and the specified values of the other parameters are given in Table III. The final numerical values of the estimated parameters are given in Table IV. Using these nu-

Table II. Parameter values chosen for *a priori* sensitivity analysis of kinetic model A

Parameters[a]	Reference values	Scaling factors	Scaled value	
$i_{o1,ref}$ (A/cm^2)	1.026×10^{-12}	10^{-12}	1.026	
$i_{o2,ref}$ (A/cm^2)	8.468×10^{-8}	10^{-9}	0.8468	
$i_{o3,ref}$ (A/cm^2)	1.896×10^{-10}	2×10^{-10}	0.948	
$\alpha_{c,1}$	0.85	1.00	0.850	
$\alpha_{c,2}$	1.00	1.00	1.00	
$\alpha_{c,3}$	0.25	1.00	0.25	
k_h (cm^3/s)	1.756×10^{-2}	2.0×10^{-2}	0.878	
$D_{HO_2^-}$ (cm^2/s)	5.00×10^{-6}	5.0×10^{-6}	1.00	
D_{O_2} (cm^2/s)	$6.698 = 10^{-6}$	6.698×10^{-6}	1.00	
Solution properties	O_2	HO_2^-	Na^+	OH^-
$c_{i,ref}$ (mol/cm^3)	2.389×10^{-7}	4.264×10^{-9}	0.0065	0.0065
D_i (cm^2/s)	7.500×10^{-6}	5.00×10^{-6}	1.975×10^{-5}	9.717×10^{-6}
Other properties	Reaction [1]	Reaction [2]	Reaction [2]	Reaction [4]
U_j^θ (V)	0.401	−0.0649	0.870	
n_j	4	2	2	
p				1
$\rho_o = 0.001$ kg/cm^3	$T = 298.15$ K	$\Omega = 1600$ rpm	$\nu = 0.042$ cm^2/s	
$A = 0.196$ cm^2	$U_{re}^\theta = 0.109$ V			

[a]To be determined by parameter estimation technique.

Table III. Initial parameter values for analysis of the data of Yeager *et al.* (28) for O_2 reduction on carbon by the parameter estimation procedure

Parameters	Reaction [2]	Reaction [3]		
$\alpha_{c,j}$	0.500	0.140		
$i_{oj,ref}$ (A/cm^2)	9.0×10^{-5}	5.4×10^{-7}		
$U_j^{\theta,a}$ (V)	−0.0649	0.870		
n_j	2	2		
Solution properties	O_2[b]	HO_2^-	Na^+	OH^-
$c_{i,ref}$ (mol/cm^3)	2.523×10^{-7}	1.600×10^{-5}	0.00402	0.004
D_i (cm^2/s)	$8.80) \times 10^{-5}$	6.300×10^{-6}	1.20×10^{-5}	1.350×10^{-5}
ρ_o = 0.001 kg/cm^3	T = 298.15 K	Ω = 12,000 rpm	A = 0.180 cm^2	ν = 0.013[c] cm^2/s

[a]Values taken from (29).
[b]Values taken from (30).
[c]Values taken from (31).

Table IV. Comparison of estimated and calculated parameters for the data of Yeager *et al.*[a]

Parameter	Model E	Model D	Calculated values[b]
$i_{o2,ref}$ (A/cm^2)	$(9.613 \pm 0.132) \times 10^{-5}$	$(9.922 \pm 0.081) \times 10^{-5}$	8.229×10^{-5}
$i_{o3,ref}$ (A/cm^2)	—	$(5.879 \pm 0.185) \times 10^{-7}$	—
$\alpha_{c,2}$	0.570 ± 0.020	0.550 ± 0.013	0.500
$\alpha_{c,3}$	—	0.060 ± 0.010	—
$D_{HO_2^-}$ (cm^2/s)	$(6.893 \pm 0.013) \times 10^{-6}$	$(6.887 \pm 0.081) \times 10^{-6}$	—
D_{O_2} (cm^2/s)	$(7.345 \pm 0.301) \times 10^{-6}$	$(7.399 \pm 0.010) \times 10^{-6}$	7.087×10^{-6}
SSE	2.333×10^{-10}	2.441×10^{-10}	
MSE	7.526×10^{-12}	8.417×10^{-8}	

[a]See Ref. (28).
[b]Using Tafel and Levich equations.

merical values of the parameters obtained from the parameter estimation procedure for models E and D, pairs of i *vs.* E_{appl} values were generated from the model for oxygen reduction (26) for comparison to the experimental values. The results are plotted in Fig. 4. A visual inspection of this figure indicates that there is no appreciable difference between the fits of the two models D and E to the data. Quantitatively, the values of the sum of the squares of the deviations, SSE, in Table IV of the two models from the experimental data are almost the same; so also are the mean square errors, *i.e.*, both very small. To provide a statistical basis for distinguishing between the two models, the b^* values for models D and E were computed in accordance with Wilks procedure (24, 25, 21) and were found to be 0.51 and 0.49, respectively. This result shows that models D and E fit the data equally well. Furthermore, the two b^*'s were tested on the basis of Eq. [27] to determine if there exists any significant difference between the fits of the two models to the data. The computed t value was found to be 0.53, which is far less than the tabulated value of 1.69 from the t distribution (32). This again supports the contention that there is no significant difference between the fits of the two models to the data.

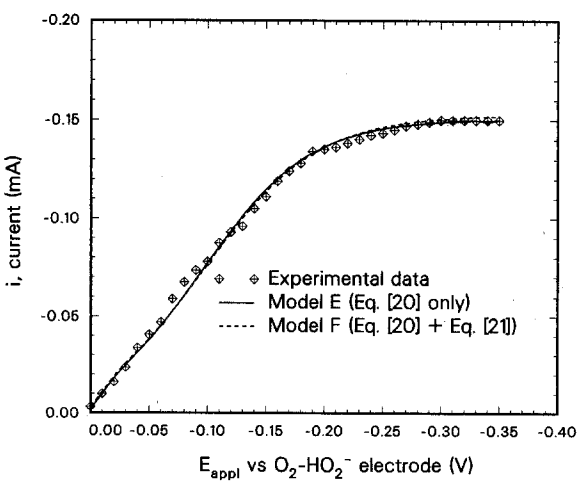

Fig. 4. Kinetics of the O_2^- HO_2^- couple on carbon. Data of Yeager *et al.* (26).

Yeager *et al.* (28) claim that there was no appreciable contribution by reaction [30] to the net current density and, on the basis of this, concluded that model *E* was the appropriate model to describe the experimental data. Considering the fact that initially there was an appreciable amount of HO_2^- in the solution, the contribution of reaction [30] to the total current would be expected to be fairly substantial. However, at the optimum values of the parameters for model D, the partial current due to reaction [30] is on the average less than 2% of the total current over the entire range of the applied potential. This observation supports the contention of Yeager *et al.* (28) that the contribution of reaction [30] to the overall current over the potential range considered is negligible. Therefore, model E can conveniently be chosen to describe the data.

Comparison of the model estimates of the kinetic parameters with the parameters evaluated from the polarization curve by conventional techniques (Tafel plots and the Levich equation) is displayed in Table IV. The calculated (from Tafel plots and the Levich equation) and the estimated parameters agree reasonably well within the limits of experimental error. The implication of the above results is that for a reaction system in which the data can be described by a fairly simple reaction model such as kinetic model E, conventional techniques such as Tafel plots are adequate in providing accurate estimates of the relevant parameters. However, as the reaction model becomes more complicated, conventional techniques become inadequate. Consequently, more sophisticated techniques, such as the parameter estimation procedure outlined in this paper, have to be applied in order to obtain more accurate estimates of the parameters. The examples that follow confirm the limitations of conventional techniques.

O_2 reduction on graphite in 1M NaOH solution.—The next set of experimental data analyzed with the parameter estimation procedure is that of Lovrecek *et al.* (33) for O_2 reduction on a graphite electrode in 1*M* NaOH solution. The

Table V. Initial parameter values for analysis of the data of Lovrecek *et al.* (33) on O_2 reduction at graphite electrode by the parameter estimation technique

Parameters	Reaction [2]	Reaction [3]		
$\alpha_{c,j}$	1.327	0.276		
$i_{oj,ref}$ (A/cm^2)	5.40×10^{-7}	2.308×10^{-12}		
$U_j^{\theta,a}$ (V)	−0.0649	0.870		
n_j	2	2		
Solution properties	O_2	HO_2^-	Na^+	OH^-
$c_{i,ref}$ (mol/cm^3)	$8.40 \times 10^{-7,b}$	4.152×10^{-9}	0.001	0.001
D_i (cm^2/s)	1.500×10^{-5}	9.30×10^{-6}	1.334×10^{-5}	5.200×10^{-5}
$\rho_o = 0.001$ kg/cm^3	$T = 298.15$ K	$\Omega = 300$ and 2400 rpm	$\nu = 0.012^c$ cm^2/s	$A = 0.274$ cm^2

[a]Values taken from (29).
[b]Value taken from (33).
[c]Value taken from (31).

Table VI. Comparison of parameter values for the data of Lovrecek *et al.*[a]

$\Omega = 300$ rpm			
Parameter	Model values	Calculated values[b]	Lovrecek's values
$i_{o2,ref}$ (A/cm^2)	$(5.342 \pm 0.196) \times 10^{-7}$	5.836×10^{-7}	
$i_{o3,ref}$ (A/cm^3)	$(2.297 \pm 0.164) \times 10^{-12}$	7.393×10^{-14}	
$\alpha_{c,2}$	1.325 ± 0.031	1.273	0.897
$\alpha_{c,3}$	0.280 ± 0.011	0.436	
$D_{HO_2^-}$ (cm^2/s)	$(9.896 \pm 0.124) \times 10^{-6}$		
D_{O_2} (cm^2/s)	$(1.538 \pm 0.032) \times 10^{-5}$	1.496×10^{-5}	1.790×10^{-5}
$\Omega = 2400$ rpm			
Parameter	Model values	Calculated values[b]	Lovrecek's values
$i_{o2,ref}$ (A/cm^2)	$(5.474 \pm 0.602) \times 10^{-7}$	1.123×10^{-5}	
$i_{o3,ref}$ (A/cm^2)	$(1.505 \pm 0.710) \times 10^{-12}$	6.244×10^{-14}	
$\alpha_{c,2}$	1.332 ± 0.070	0.857	0.642
$\alpha_{c,3}$	0.275 ± 0.012	0.448	
$D_{HO_2^-}$ (cm^2/s)	$(9.654 \pm 0.504) \times 10^{-6}$		
D_{O_2} (cm^2/s)	$(1.531 \pm 0.051) \times 10^{-5}$	1.496×10^{-5}	1.790×10^{-5}

[a]See Ref. (33).
[b]Using Eq. [32] and [33].

model proposed by Lovrecek *et al.* (33) for this system was model D; the 2-step reduction of O_2 to OH^- via a peroxide intermediate. The basis for the choice of this model was the two well-defined limiting current regions on the polarization curve. The current densities in the limiting regions appearing on the polarization curve agreed with the theoretical limiting current densities for the $2e^-$ and $4e^-$ processes for O_2 reduction. Consequently, model D was used to fit the experimental data, in an attempt to establish some validity for this alternative procedure for electrokinetic data analysis. The initial values of parameters to be estimated: $i_{o2,ref}$, $\alpha_{c,2}$, D_{O_2}, $i_{o3,ref}$, and $\alpha_{c,3}$ were obtained on the basis of conventional analysis of the data via Tafel plots and the Levich equation. Initial guesses of the parameters to be estimated and the specified values of the other parameters are given in Table V.

Figure 5 shows a fit of the two-step peroxide model to the data at 300 rpm and 2400 rpm. The fit of the model to the data is excellent over nearly the whole range of the polarization curve. Table VI presents a comparison of the estimated, calculated, and reported parameters as discussed next.

The "calculated" exchange current densities and transfer coefficients at each rotation speed shown in Table VI were obtained from the Tafel equation corrected for mass transport effects as given by the following expression (34)

$$\eta = \frac{2.303RT}{\alpha_c \mathbf{F}} \log \frac{i_o}{i_L} - \frac{2.303RT}{\alpha_c \mathbf{F}} \log \frac{i}{i_L - i} \qquad [32]$$

The diffusion coefficient of O_2 was calculated from the slope of the plot of $1/i$ *vs.* $1/\sqrt{N}$ in Eq. [33]

$$\frac{1}{i} = \frac{1}{i_k} + \frac{1}{B\sqrt{N}} \qquad [33]$$

where i_k represents the current density in the absence of any mass transfer effects, $B = 0.62n\mathbf{F}D_{O_2}^{2/3}\nu^{-1/6}(2\pi/60)^{1/2}c_{O_2}$ and N is the rotation speed of the electrode in rpm. Comparison of the parameters in Table VI indicates that the calculated exchange current density and the apparent transfer coefficient for the first wave agree reasonably well

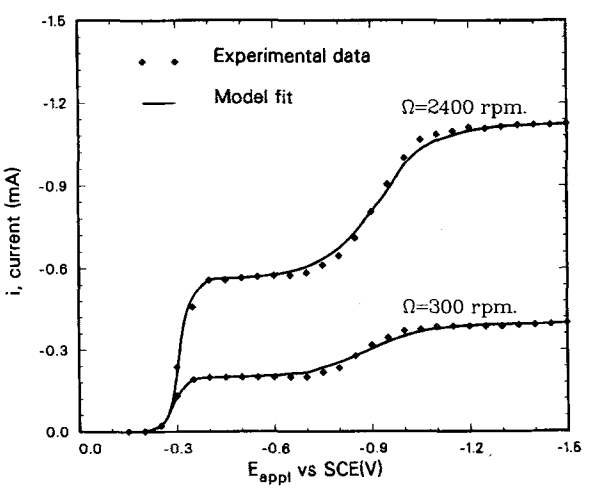

Fig. 5. Oxygen reduction on graphite in 1M NaOH solution. Data of Lovrecek, *et al.* (31).

Table VII. Initial parameter values for analysis of the data of Brezina *et al.* (33) on O_2 reduction at silver electrode by the parameter estimation technique

Parameters	Reaction [1]	Reaction [2]	Reaction [3]	Reaction [4]
$\alpha_{c,j}$	0.78	1.00	0.150	
$i_{oj,ref}$ (A/cm^2)	2.80×10^{-12}	3.00×10^{-10}	9.30×10^{-11}	
$U_j^{\theta,a}$ (V)	0.401	−0.0649	0.870	
n_j	4	2	2	
p, k_h cm/s			1, 0.0101	
Solution properties	O_2[b]	HO_2^-	K^+	OH^-
$c_{i,ref}$ (mol/cm^3)	1.197×10^{-6}	2.082×10^{-10}	1.27×10^{-4}	1.27×10^{-4}
D_i (cm^2/s)	1.85×10^{-5}	9.300×10^{-6}	1.957×10^{-5}	5.260×10^{-5}
$\rho_0 = 0.001$ kg/cm^3	$T = 298.15$ K	$\Omega = 512$ rpm	$\nu = 0.0101$[c] cm^2/s	

[a]Values taken from (29).
[b]Values taken from (30).
[c]Value taken from (31).

with the estimated values at the lower rotation speed of 300 rpm. On the other hand, there is a large disparity between the calculated and estimated values for the apparent transfer coefficients and the exchange current densities for the two reduction waves at 2400 rpm and for the second reduction wave at 300 rpm. The reason for the apparent discrepancy in these values might be due to coupling of the two reactions. With the parameter estimation procedure, the two reactions are considered simultaneously; whereas with conventional data analysis approach, it is not possible to handle both reactions simultaneously. Therefore, the parameters obtained from the conventional technique are not truly characteristic of the individual charge-transfer reactions. The calculated diffusion coefficient for oxygen is in excellent agreement with the parameter estimated coefficient. This value agrees with the literature value of 1.525×10^{-5} cm^{-2}/s obtained by Gubbins and Walker (35) for O_2 reduction in 4 w/o KOH solution (corresponding to 1*M* NaOH solution), but not with the value presented by Lovrecek *et al.* (33). Further comparison of the parameters indicates that the parameters obtained from the parameter estimation technique at the two rotation speeds are in close agreement with each other within the limits of experimental error.

O_2 reduction on silver electrode in 0.127M KOH solution.— It has been well documented in the literature that O_2 reduction on silver electrode occurs by either the parallel or consecutive mechanism (36). Silver is also known to be a good peroxide decomposition catalyst (37, 38).

The experimental data of Brezina *et al.* (39) were fitted with various models for O_2 in order to determine which model best describes the data. The models considered are the comprehensive model (model A) with a first-order catalytic peroxide decomposition rate, the parallel mechanism without peroxide decomposition (model B), the sequential mechanism with and without peroxide decomposition (models C and D), and the direct $4e^-$ mechanism (model G). Brezina *et al.* (39) found the limiting current density at −1.2V to correspond to the value predicted by the Levich equation for the $4e^-$ mechanism for O_2 reduction. On the basis of latter and using the values of $c_{O_2} = 1.197 \times 10^{-6}$ mol/cm^3 and $D_{O_2} = 1.85 \times 10^{-5}$ cm^2/s from the data of Davis *et al.* (30) and for $n = 4$ and $\nu = 0.0101$ cm^2/s (31), the effective surface area of the electrode was calculated to be 0.0076 cm^2 as compared with the measured value of 0.031 cm^2. The initial parameter values for evaluating the optimum parameters by the parameter estimation procedure are listed in Table VII. The sum of squares of the residuals for each model and the corresponding mean square error are listed in Table VIII. The disparity in the mean square errors of these models indicates significant differences in the fits of the models to the experimental data. The Wilk's test was applied to the five models in an attempt to determine which model best fits the data. The b^* values indicate that models A and B are the best models that describe the data. Models A and B were then tested as described earlier using the t value in Eq. [27] in order to determine which of the two regression equations fit the data better. The calculated t value was found to be 32.33, which is far greater than the tabulated value (32) of 1.714 at 10% significance level. This implies that the b^* values for models A and B are significantly different from each other and that model A is a better fit to the experimental data.

Table VIII. Residual sum of squares of various models tested. Data of Brezina *et al.*[a]

Model	SSQ	MSE	b^*
A	1.271×10^{-11}	7.474×10^{-13}	0.72
B	2.013×10^{-10}	1.181×10^{-11}	0.16
C	3.045×10^{-10}	1.603×10^{-11}	0.05
D	1.357×10^{-9}	6.786×10^{-11}	0.072
G	8.336×10^{-9}	3.624×10^{-10}	0.002

[a]See Ref. (39).

The fit of model A to the experimental data is shown in Fig. 6. Visual inspection confirms that the model fit to the data is excellent. The optimum parameter values that produced this fit are given in Table IX. Brezina *et al.* (39) showed from their experiments on oxygen reduction at silver electrode that the final reduction product was water, and this was formed at the limiting current of both the first and second reduction waves. The intermediate product in these processes was peroxide and the dip in the polarization curve was attributed to the conversion of peroxide to water being hindered in this potential range by possibly hydrogen evolution process. The results presented here confirm the claim of Brezina *et al.* (39) that the reduction of O_2 on Ag electrode involves the parallel mechanism. The results presented here also indicate that the final reduction product observed at the limiting current of the first wave is due predominantly to reaction [28], the direct $4e^-$ process,

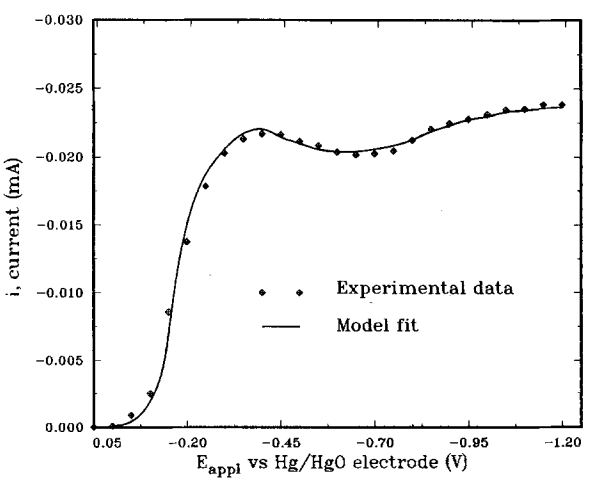

Fig. 6. Reduction of oxygen on silver in 0.127M KOH solution at 512 rpm. Data of Brezina *et al.* (37).

Table IX. Optimum parameters values for the best model fit to the data of Brezina[a] for O_2 reduction on Ag in 0.127M KOH solution

Parameter	Optimum values
$i_{o1,ref}$ (A/cm^2)	$(2.766 \pm 0.266) \times 10^{-10}$
$i_{o2,ref}$ (A/cm^2)	$(2.946 \pm 0.321) \times 10^{-8}$
$i_{o3,ref}$ (A/cm^2)	$(9.080 \pm 0.276) \times 10^{-11}$
$\alpha_{c,1}$	0.785 ± 0.018
$\alpha_{c,2}$	1.010 ± 0.066
$\alpha_{c,3}$	0.149 ± 0.010
k_h (cm/s)	$(8.256 \pm 0.048) \times 10^{-3}$
$D_{HO_2^-}$ (cm^2/s)	$(7.931 \pm 0.084) \times 10^{-6}$
D_{O_2} (cm^2/s)	$(1.876 \pm 0.098) \times 10^{-5}$

[a]See Ref. (39).

and that observed at the second wave is due mainly to reaction [30], the peroxide process. The depression in the polarization curve can be attributed to the competition between reactions [28] and [29] for O_2 species at the electrode surface (see Ref. (26)). The role played by hydrogen evolution or the surface oxides of silver on the reduction process is not fully understood. However, it is likely that these processes affect the exchange current densities and the transfer coefficients for the parallel reactions in Eq. [28] and [29] and reduce their magnitudes to levels that enhance the formation of the dip in the polarization curve. Therefore, it can be inferred from the above analysis that under the given experimental conditions, the parallel mechanism for O_2 reduction occurs on Ag with the direct $4e^-$ process dominating at the lower to intermediate potential regions, while the sequential process dominates in the higher potential regions.

Conclusion

The technique outlined in this paper can serve as a useful tool in the analysis of electrokinetic data, particularly for complex reaction systems that have proved difficult to analyze with conventional data analysis techniques.

Manuscript submitted Aug. 10, 1987; revised manuscript received Nov. 16, 1987.

Texas A&M University assisted in meeting the publication costs of this article.

LIST OF SYMBOLS

A Electrode area, cm^2
B Levich constant
c_i concentration of species i, mol/cm^3
D_i diffusion coefficient of species i, cm^2/s
D_R diffusion coefficient of limiting reactant, cm^2/s
e_k residual error of k^{th} data point
E_{appl} applied electrode potential, V
$E_{1/2}$ half-wave potential, V
$\mathbf{F}$ Faraday's constant, 96,487 C/mol
$F(x,t)$ objective function
$f(x,t)$ dependent variable
h step-size in numerical solution technique
i_j local current density due to reaction j, A/cm^2
$i_{oj,ref}$ exchange current density due to reaction j at reference concentrations, A/cm^2
i total current density, A/cm^2
i_d diffusion limiting current density, mA/cm^2
i_k current density in the absence of mass transfer effects (see Eq. [33]), mA/cm^2
$\mathbf{I}$ identity matrix
I total current, mA
I_L limiting current, mA
I_d diffusion limiting current, mA
K_{eq} equilibrium constant for homogeneous reaction in the bulk solution
k_b backward rate constant for homogeneous reaction
k_f forward rate constant for homogeneous reaction
k_h rate constant for non-charge-transfer reaction at electrode surface
m number of charge transfer reactions at electrode surface
nr number of reactions at the electrode
N_i flux of species i, mol/cm^{2}s
$\mathbf{N}$ Levenberg-Marquardt approximation to the Hessian
N number of species in the solution
n_j number of electrons transferred in reaction j
p reaction order with respect to HO_2^- species in catalytic peroxide decomposition rate equation
p_{ij} anodic reaction order for species i in reaction j
q_{ij} cathodic reaction order for species i in reaction j
$\mathbf{q}$ gradient vector of objective function
$\tilde{\mathbf{q}}$ relative sensitivity
R universal gas constant, 8.314 J/mol-K
R_i homogeneous rate of consumption of species i in bulk solution, mol/s
rpm revolution per minute
$r_{1,i}$ noncharge-transfer rate of consumption of species i at by reaction 1 at electrode surface, mol/cm^{2}s
s_{ij} stoichiometric coefficient of species i in reaction j
T absolute temperature, K
u_i mobility of species i, cm^{2}mol/J-s
U_{re}^{θ} standard potential of reference electrode, V
U_j^{θ} standard electrode potential for reaction j, V
w_k weight attached to the k^{th} observed value
$\mathbf{x}$ vector of parameters to be estimated
z_i charge of species i

Greek

γ percent significance level
αn apparent transfer coefficient for reaction j
$\alpha_{a,j}$ apparent anodic transfer coefficient for reaction j
$\alpha_{c,j}$ apparent cathodic transfer coefficient for reaction j
δ_D diffusion layer thickness, cm
ϵ_i degree of dissociation or association of species i
λ_o Levenberg-Marquardt parameter
ρ_o pure solvent density, kg/cm^3
ρ^j a scalar at the j iteration in the parameter estimation routine
Φ potential in the solution, V
Φ_{met} potential of working electrode, V
Φ_{re} potential in the bulk solution at the location of the reference electrode, V
Φ_o potential in the solution just beyond the double layer, V
η_j overpotential of reaction j corrected for ohmic drop in the solution and measured with respect to a reference electrode of a given kind in a solution at the reference concentrations, V
μ_i stoichiometric coefficient of species i in the homogeneous reaction
ν_j reaction rate for elementary reaction j
ν kinematic viscosity, cm^2/s
ξ dimensionless distance from electrode surface
Ω rotation speed, rad/s
γ_{ij} reaction order of species i in reaction j

Subscripts

o at the electrode surface
j reaction, j
re reference electrode
ref reference conditions
∞ in the bulk solution

REFERENCES

1. J. D. E. McIntyre, *J. Phys. Chem.*, **73,** 4102 (1969).
2. Z. Nagy, R. H. Land, G. K. Leaf, and M. Minkoff, *This Journal,* **132,** 2626 (1985).
3. V. G. Levich, "Physicochemical Hydrodynamics," Prentice-Hall, Englewood Cliffs, New Jersey (1962).
4. P. K. Adanuvor, R. E. White, and S. E. Lorimer, *This Journal,* **134,** 625 (1987).
5. R. Caban and T. Chapman, *ibid.*, **124,** 1371 (1977).
6. S. Yen and T. W. Chapman, *Chem. Eng. Commun.*, **38,** 159 (1985).
7. S. Pons, in "Electroanalytical Chemistry," Vol. 3, A. J. Bard, Editor, p. 276, Marcel Dekker, New York (1984).
8. T. Meites and L. Meites, *Talanta,* **19,** 1131 (1972).
9. V. Gorodetskii, K. A. Mishenina, V. V. Losev, A. N. Grimberg, and G. M. Ostrovskii, *Sov. Electrochem.*, **4,** 39 (1968).
10. Zh. L. Vert and V. F. Pavlova, *ibid.*, **21,** 1096 (1986).
11. L. Degreve, O. L. Bottecchia, and J. F. C. Boodts, *J. Electroanal. Chem.*, **206,** 81 (1986).
12. Z. Nagy, *ibid.*, **129,** 1943 (1982).
13. Z. Nagy, *Electrochim. Acta,* **26,** 671 (1981).
14. Y. Bard, "Nonlinear Parameter Estimation," Academic Press, London, New York (1976).
15. D. M. Himmelblau, "Applied Nonlinear Programming," McGraw-Hill Book Co., New York (1972).
16. M. A. Tarasevich, A. Sadkowski, and E. Yeager, in "Comprehensive Treatise of Electrochemistry," Vol.

7, B. E. Conway, J. O'M Bockris, E. Yeager, S. U. M. Khan, and R. E. White, Editors, p. 301, Plenum Press, New York (1983).
17. R. E. White and S. E. Lorimer, *This Journal*, **130**, 1096 (1983).
18. Y. V. Pleskov and V. Y. Filinovskii, "The Rotating Disc Electrode," Consultants Bureau, New York (1976).
19. J. S. Newman, "Electrochemical Systems," Prentice-Hall, Englewood Cliffs, New Jersey (1973).
20. P. K. Adanuvor, Ph.D. Dissertation, Texas A&M Univ., College Station, Texas (1987).
21. D. M. Himmelblau, "Process Analysis by Statistical Methods," John Wiley & Sons, Inc., New York (1968).
22. R. E. White, C. W. Walton, and D. J. Wolfe, *Chem. Eng. Commun.*, **38**, 229 (1985).
23. The Editorial Board, "The IMSL Library," Vol. 4, p. ZXSSQ-1, Marcel Dekker, Houston (1982).
24. S. S. Wilks, *Ann. Math. Stat.*, **17**, 257 (1946).
25. E. J. Williams, "Regression Analysis," John Wiley and Sons Inc., New York (1959).
26. P. K. Adanuvor and R. E. White, *This Journal*, **134**, 1093 (1987).
27. J. O'M. Bockris and A. K. N. Reddy, "Modern Electrochemistry," Vol. 2, Plenum Press, New York (1977).
28. E. Yeager, P. Krouse, and K. V. Rao, *Electrochim. Acta*, **9**, 1054 (1964).
29. J. P. Hoare, "Standard Potentials in Aqueous Solution," A. J. Bard, R. Parson, and J. Jordan, Editors, Marcel Dekker, New York (1985).
30. R. E. Davis, G. L. Horvath, and C. W. Tobias, *Electrochim. Acta*, **12**, 287 (1967).
31. A. V. Wolfe, M. G. Brown, and P. G. Prentiss, in "CRC Handbook of Chemistry and Physics," 63rd Edition, R. C. Weast, Editor, p. D227, CRC Press, Inc., Florida (1982).
32. R. A. Fischer and F. Yates, "Statistical Tables," Oliver and Boyd, Edinburgh, Scotland (1938).
33. B. Lovrecek, M. Batinic, and J. Caja, *Electrochim. Acta*, **28**, 685 (1983).
34. A. J. Bard and L. R. Faulkner, "Electrochemical Methods," John Wiley and Sons, Inc., New York (1980).
35. K. E. Gubbins and D. Walker, *This Journal*, **112**, 469 (1965).
36. P. Fischer and J. Heitbaum, *J. Electroanal. Chem.*, **112**, 281 (1980).
37. E. L. Littauer and K. C. Tsai, *Electrochim. Acta*, **24**, 681 (1979).
38. K. Goszner, D. Korner, and R. Hite, *J. Catal.*, **25**, 245 (1972).
39. M. Brezina, J. Korta, and M. Musilova, *Collect. Czech. Chem. Commun.*, **33**, 3397 (1968).

Electrodeposition of H^+ on Oxide Layers at Pyrite (FeS_2) Surfaces

K. K. Mishra and K. Osseo-Asare

Department of Materials Science and Engineering, The Pennsylvania State University, University Park, Pennsylvania 16802

ABSTRACT

The electrochemical behavior of pyrite (FeS_2) has been studied in 1 mol dm^{-3} $HClO_4$ solution in the potential range of −350-300 mV (SCE). Reversible surface processes are observed in this potential region. The electrochemical i-V behavior is found to be dependent upon the amount of surface oxide below a monolayer that is present and on the *p*H. These surface processes are attributed to the electroadsorption/desorption of H^+ on a surface oxide layer.

There are several reasons for the current interest in the electrochemical behavior of pyrite and other sulfide minerals (1-17). Among these reasons are the use of metal sulfides in high energy batteries (1), solar energy applications (2-4), the need to treat low grade and complex sulfide ores by direct leaching (5-8), the possibility of direct electrowinning of metals from sulfide ores (9), and the need to desulfurize coal (10-11).

In a pioneering study, Peters and Majima (7) carried out an electrochemical investigation of pyrite in 1 mol dm^{-3} perchloric acid. They obtained an open-circuit potential of 0.62V (SHE), which differs significantly from the thermodynamic value of 0.34V (SHE) which is the standard potential for Eq. [1]. The discrepancy between the theoretical potential and the observed open-circuit potential has been attributed to the presence of a passive film on the pyrite surface (17, 18). The nature of this film is yet to be determined (17), although it has been suggested that in acidic solutions the formation of a surface layer of sulfur according to the Eq. [1] limits the rate of dissolution (18). The elemental sulfur forming and the sulfate forming reactions are given by Eq. [1] and [2], respectively (8, 15, 17)

$$FeS_2 = Fe^{2+} + 2S + 2e^- \qquad [1]$$

$$E_1 = 0.34 + 0.0295 \log a_{Fe^{2+}}$$

$$FeS_2 + 8H_2O = Fe^{3+} + 2SO_4^{2-} + 16H^+ + 15e^- \qquad [2]$$

$$E_2 = 0.389 - 0.063\ pH + 0.0039 \log a_{Fe^{3+}} + 0.0079 \log a_{SO_4^{2-}}$$

There is general agreement that at lower potentials the anodic dissolution takes place according to Eq. [1] and that dissolution via Eq. [2] predominates at higher potentials (7, 17).

The surface reactivity of pyrite was studied by Conway *et al.* (16) who observed two reversible peaks on the cyclic voltammograms. These peaks were attributed to reversible monolayer surface processes. The following reaction was suggested as an initial step, although the processes were not fully identified

$$S_2^{2-}\ (\text{lattice}) + 2e^- = 2S^{2-}\ (\text{lattice}) \qquad [3]$$

Similar peaks were also observed by Biegler *et al.* (6), and even though the origin of these peaks was not identified, the following reaction was believed to be associated with these surface processes (6)

$$FeS_2 + 2xH^+ + 2xe^- = FeS_{2-x} + xH_2S \qquad [4]$$

In this communication we report that these peaks are associated with the electroadsorption of hydrogen on oxide films over pyrite.

Experimental

Pyrite electrode.—Pyrite crystals were obtained from Wards Scientific Establishment (Rochester, NY). The electrodes were made by cutting the pyrite sample into small disk-shaped pieces (area = 1 cm^2). Gold was coated on one side of the disk and contact was found to be ohmic. The disks were glued onto a plexiglass holder. The electrical connections were made internally from the back side by a screw-fitting arrangement. The remaining space between the sides of the sample and the holder was filled with